

## Hydraulic jumps on rough and smooth beds: aggregate approach for horizontal and adverse-sloped beds

STEFANO PAGLIARA (IAHR Member), Professor, *DESTEC - Department of Energy Engineering, Systems, Land and Construction, University of Pisa, Pisa, Italy*

*Email: s.pagliara@ing.unipi.it (author for correspondence)*

MICHELE PALERMO (IAHR Member), Researcher, *DESTEC - Department of Energy Engineering, Systems, Land and Construction, University of Pisa, Pisa, Italy*

*Email: michele.palermo@ing.unipi.it*

*Running Head: Hydraulic jumps on rough and smooth beds*

# Hydraulic jumps on rough and smooth beds: aggregate approach for horizontal and adverse-sloped beds

## ABSTRACT

Hydraulic jumps, which frequently occur in hydraulic structures, have been extensively studied over the last century. However, only few studies have evaluated hydraulic jumps in flows over rough beds and there are no studies that considered air entrainment effect on conjugate depths. The present paper reports the results of an experimental investigation of hydraulic jump properties in flows over adverse-sloped rough beds, including the effect of air entrainment. Furthermore, a semi-theoretical predictive relationship is proposed to estimate jump characteristics for a wide range of hydraulic and geometric conditions covering both rough and smooth beds.

*Keywords:* aerated flows; bubble dynamics; bed roughness; drag coefficient; friction factor; hydraulic jumps; hydraulic models; hydraulic resistance;

## 1. Introduction

A hydraulic jump is a standing wave phenomenon that occurs when supercritical flow changes to subcritical. Hydraulic jumps can often be observed in nature as well as in man-made flow structures and therefore they have been extensively studied and analysed over the last century. There are many contributions in the literature regarding the estimation of the main jump parameters (e.g., sequent depths ratio, roller length, jump length, etc.) and their energy dissipative properties for a wide range of hydraulic and geometric configurations (e.g., Paterka, 1983).

Early studies conducted in rectangular horizontal smooth-walled channels (Bakmeteff, 1932) and application of the momentum principles led to the well-known Bélanger's equation, assuming uniform velocity and hydrostatic pressure distributions upstream and downstream of the hydraulic jump and negligible boundary flow resistance. Harleman (1959) showed that the sequent depths ratio values are lower for high upstream Froude numbers than predicted by Bélanger's equation. Gill (1980) also found that the sequent depth ratio is over-estimated if the channel boundary flow resistance is neglected. Therefore, alternative methods for determining sequent depth values in horizontal, smooth-walled channels have been proposed that account for additional parameters (e.g., Carollo, Ferro, & Pampalone, 2009; Leuthesser & Kartha, 1972; McCorquodale & Khalifa, 1983; Rajaratnam, 1965; Wu & Rajaratnam 1995).

The influence of bed flow resistance on hydraulic jump characteristics in horizontal channels has been evaluated using either semi-theoretical or empirical approaches. Leuthesser & Schiller (1975) analysed the characteristic lengths of hydraulic jumps

occurring on roughened horizontal beds using both spheres and strips. Hughes & Flack (1984) tested different rough-bed configurations featuring strip roughness materials and gravels of various sizes. Ead & Rajaratnam (2002) analyzed hydraulic jumps on a corrugated bed and identified substantial axial velocity profile similitude at different cross sections of the hydraulic jump. Carollo, Ferro, & Pampalone (2007) analysed the hydraulic jump properties on several horizontal rough-bed configurations; they proposed a new solution of the momentum equation for the sequent depth ratio and empirical relationships for the roller length. Namely, they showed that sequent depth ratio is dependent on both approaching flow Froude number and relative roughness. Pagliara, Lotti, & Palermo (2008) conducted a similar investigation analyzing the effect of channel bed material non-uniformity, proposing empirical relationships to predict the main hydraulic jump characteristics.

More recently, Bhuiyan, Habibzadeh, Rajaratnam, & Zhu (2011) and Afzal, Bushra, & Seena, (2011) conducted a series of experiments on turbulent submerged offset jets and turbulent rough-bed hydraulic jumps. They concluded that the characteristic lengths of a rough-bed hydraulic jump can be derived adopting a modified upstream Froude number. Nevertheless, none of the mentioned studies conducted in the presence of rough beds took into consideration the air concentration effect on the conjugate depths, even if, especially for high relative roughness, it can affect effective water depths.

Other aspects that have been extensively studied include the effect of channel geometry (channel shape and slope) and the presence of a downstream sill on hydraulic jump properties. In particular, hydraulic jump characteristics in a flow on a smooth adverse-sloped bed were analysed by Stevens (1942), Okada & Aki (1955), Rajaratnam (1966), Rajaratnam (1967) and McCorquodale & Mohamed (1994). McCorquodale & Mohamed (1994) proposed a theoretical approach based on conservation of momentum principles to estimate hydraulic jump characteristics and found that the stability of a hydraulic jump on an adverse slope is also depending on the upstream Froude number. The presence of a sill increases hydraulic jump stability for both horizontal (Hager & Bretz, 1988; Ohtsu, 1981; Ohtsu, Yasuda, & Yamanaka, 1991) and adverse-sloped beds (Pagliara & Peruginelli, 2000). In particular, Pagliara & Peruginelli (2000) conducted a series of experimental tests with and without a sill, varying the bed slope from 0 to -20% (adverse slope). They concluded that the presence of the sill stabilizes the hydraulic jump location and presented a general equation for predicting the characteristic hydraulic jump lengths.

More recently, Jan & Chang (2009) conducted a comprehensive analysis of the hydraulic jump properties in an inclined rectangular chute contraction, proposing a theoretical equation to predict the sequent depth ratio in which a modified approach flow Froude number was adopted.

The present study aims to furnish general predicting relationships for hydraulic jump characteristics, valid for a wide range of channel geometric and bed roughness conditions. Experimental tests on adverse-sloped rough beds were conducted taking into consideration air concentrations both upstream and downstream of the hydraulic jump in order to estimate the effective conjugate water depths.

No studies were found in the literature evaluating the effective flow depths in relation to hydraulic jumps occurring on adverse-sloped rough beds and accounting for air concentration influences. A semi-theoretical approach is used to develop a novel general relationship for the conjugate depth ratio. The proposed equation is validated using additional data derived from previous studies, featuring both smooth adverse-sloped beds and rough horizontal beds.

## 2. Experimental setup and methodology

The experiments were conducted at the Hydraulic Laboratory of the University of Pisa, Pisa, Italy. Tests were carried out in two rectangular channels. Namely, Channel 1 has the following geometric characteristics: 0.345 m wide, 6.0 m long and 0.5 m high. It was used for experimental tests with bed slope  $i = -0.05$ . Additional validation tests were conducted in Channel 2 (0.35 m wide, 6.0 m long and 0.7 m high, bed slope  $i = -0.1$ ).

For Channel 1, the base materials tested were *E2*, *E3* and *E4* (Pagliara et al., 2008), with granulometric characteristics as:  $d_{50} = 6.26$  mm,  $d_{90} = 7.48$  mm and non-uniformity coefficient  $\sigma = (d_{84}/d_{16})^{0.5} = 1.18$  for material *E2*;  $d_{50} = 19.93$  mm,  $d_{90} = 23.7$  mm and  $\sigma = 1.14$  for material *E3*;  $d_{50} = 30.62$  mm,  $d_{90} = 33.30$  mm and  $\sigma = 1.08$  for material *E4*. For Channel 2, experiments were conducted using bed material *E3*, glued on steel sheets.

Tests were conducted by varying the downstream water depth and the inflow conditions. In the tested range of parameters (upstream Froude numbers varying between 2 and 9.5), the hydraulic jump was quite stable, especially for high relative roughness conditions, in contrast to the smooth-bed case. In addition, for adverse-sloped beds, the presence of the rough bed caused appreciable air entrainment in the flow, as also observed by Pagliara, Carnacina, & Roshni (2010). Thus, the effective flow depths and the subsequent sequent depth ratio is depending both on the air concentration upstream and downstream of the hydraulic jump and on the bed characteristics.

For bed materials *E3* and *E4*, a rooster tail formation was observed when the upstream relative roughness  $k_s/y_1 < 1$ , where  $y_1$  is the effective upstream hydraulic jump depth and  $k_s = d_{65}$  (Fig. 1), i.e., the base material diameter for which 65% is finer (Hughes & Flack,

1984; Pagliara et al., 2008). In the presence of rough adverse-sloped beds, the effect of air entrainment on hydraulic jump flow depths has not previously been investigated.

Air water flow properties were measured using a USBR single-tip conductivity probe (Fig. 2), which was aligned against the flow direction (Pagliara et al., 2010). Consistent with the definition used by Hughes & Flack (1984), Pagliara et al. (2008), Pagliara et al. (2010), the effective top  $ET$  of the channel bed is set at  $0.2k_s$  below an average level of bed material tops (i.e., the physical top  $PT$ ). The rough bed height values were measured both transversally and longitudinally, in a mesh  $1\text{ cm} \times 1\text{ cm}$ , using a point gauge with  $\pm 0.1\text{ mm}$  precision and then the obtained data were used to determine  $ET$  and  $PT$ . Figure 1 shows a sketch of a hydraulic jump occurring on an adverse-sloped rough bed, and illustrates key geometric parameters, i.e., the effective upstream and downstream depths  $y_1$  and  $y_2$ , the roller length of the jump  $L_r$  (McCorquodale & Mohamed, 1994; Pagliara & Peruginelli, 2000), and the bed slope (negative)  $i$ .

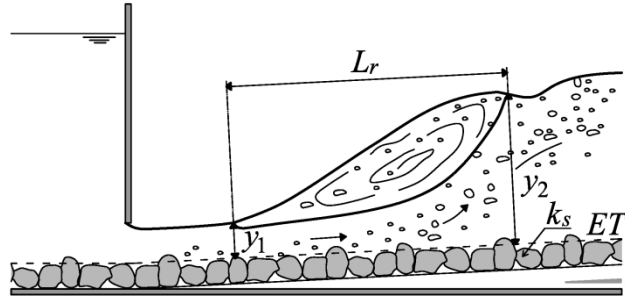


Figure 1 Sketch of a hydraulic jump on adverse-sloped rough bed

Figure 2 is a schematic sketch of the flume illustrating  $PT$  and  $ET$  elevations as well as the longitudinal and vertical coordinate system ( $x$  and  $y$ , respectively). In two-phase flow (water and entrained air), locating the “water surface” is problematic and an equivalent flow depth ( $d_e$ ) is commonly used. The depth  $d_e$  represents the normal distance from the channel invert reference ( $ET$  in this case) to an elevation where the air concentration reaches 90%. Figure 2 illustrates the air concentration  $C$  and  $y_{90}$ , i.e., the distance normal to the bed from  $PT$  to where the air concentration  $C=90\%$ . According to Pagliara et al. (2010), the upstream and downstream  $d_e$  values corresponding to  $C=90\%$  can be evaluated as follows:

$$d_e = 0.2k_s + \int_{y=0}^{y=y_{90}} (1-C) dy = 0.2k_s + y_{90} (1-C_m) \quad (1a)$$

with  $C_m$  (depth-average void fraction) equal to

$$C_m = \frac{1}{y_{90}} \int_{y=0}^{y=y_{90}} C dy \quad (1b)$$

For both upstream and downstream cross-sections, three different air concentration profiles were measured at different positions (axially and at two symmetric lateral positions) and the corresponding evaluated depths were averaged in order to obtain the sequent depths  $y_1$  and  $y_2$ , respectively. The water surface was also measured using a point gauge  $\pm 0.1$  mm precise and the probe was connected to a graduate scale allowing to measure the vertical distance of the tip from the reference levels.

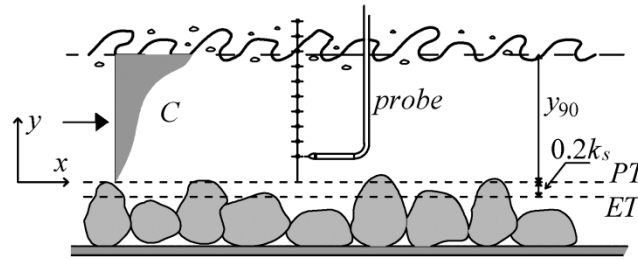


Figure 2 Location of the *ET* and *PT* levels, along with the sketch of the probe used for air concentration measurements

### 3. Semi-theoretical approach for sequent depth ratio estimation

#### 3.1. Literature review

Application of the momentum equation to a unit width in a rectangular channel with an adverse-sloped rough bed can be written as follows:

$$P_1 + M_1 + W \sin \alpha = P_2 + M_2 + F_\tau \quad (2a)$$

where  $\alpha$  is the angle of the bed slope (negative for adverse-sloped bed);  $P_j = 0.5\gamma y_j^2 \cos \alpha$  is the hydrostatic force at the beginning ( $j=1$ ) and end ( $j=2$ ) of the hydraulic jump,  $\gamma$  is the specific weight;  $M_j = \rho y_j U_j^2$  is the momentum flux in which  $U_j$  is the average velocity upstream ( $j=1$ ) and downstream ( $j=2$ ) of the hydraulic jump,  $\rho$  is water density;  $W = 0.5\gamma L K (y_1 + y_2)$  is the weight of the water in the control volume,  $L$  is the hydraulic jump length and  $K$  is a coefficient for the determination of the weight depending on the schematization of the adopted control volume. In the following, the coefficient  $K$  is assumed to be equal to 1 (McCorquodale & Mohamed, 1994; Pagliara & Peruginelli, 2000).

Carollo et al. (2007) stated that  $F_\tau$  (integrated shear stress per unit width) can be expressed as follows:

$$F_\tau = \beta (M_1 - M_2) \quad (2b)$$

where  $\beta$  is a parameter related to the momentum deficit ( $0 \leq \beta < 1$ ).

Assuming  $Y=y_2/y_1$  (sequent depth ratio) and considering Eq. (2a-b), the following general expression can be easily derived (McCorquodale & Mohamed, 1994; Pagliara & Peruginelli, 2000):

$$Y = 0.5 \left( -1 + \sqrt{1 + 8G_1^2(1 - \beta)} \right) \quad (3)$$

where

$$G_1^2 = \frac{F_1^2}{\cos \alpha - \frac{\lambda \sin \alpha}{Y - 1}} \quad (4)$$

in which  $\lambda=L/y_1$  and  $F_1=U_1/(gy_1)^{0.5}$  is the approach Froude number. Note that in the case of a hydraulic jump occurring in a flow over an adverse-sloped bed, without a sill, the length of the hydraulic jump can be assumed to be equal to the length of the roller (McCorquodale & Mohamed, 1994; Pagliara & Peruginelli, 2000). The parameter  $G_1$  is termed the ‘‘adverse jump parameter’’ and  $G_1=F_1$  for  $\alpha=0$  (i.e.,  $i=0$ ). Pagliara & Peruginelli (2000) proposed the following equation for smooth adverse-sloped beds:

$$G_1 = 3.32^{1.52i} F_1 \quad (5)$$

which is valid for  $-0.25 < i < 0$ .

### 3.2. Proposed methodology

In the present study, a procedure to estimate the momentum deficit parameter  $\beta$  was developed. Preliminary, it was proven that Eq. (5) is still valid for rough beds, as shown in Fig. 3, in which experimental values of  $G_1$  and  $F_1$  are reported along with Eq. (5) for  $i=-0.05$ . According to Eq. (2b), the momentum deficit parameter  $\beta$  is the ratio between integrated shear stress  $F_\tau$  and  $M_1-M_2$ . For a smooth channel, Leuthesser & Kartha (1972) stated that the mean value of the boundary shear stress  $\tau_{0\text{mean}}$  can be estimated from the two end points of the shear stress distribution, i.e., at the upstream and downstream ends of the jump ( $\tau_{01}$  and  $\tau_{02}$ , respectively). Namely, they stated that  $\tau_{0\text{mean}}=(\tau_{01}\tau_{02})^{0.5}$ , i.e., the geometric mean of the shear distribution end points. Hughes & Flack (1984) further extended the validity of this hypothesis to horizontal rough channels. In the present paper,  $\tau_{0\text{mean}}$  was calculated assuming the Darcy friction factors  $f_1$  and  $f_2$  (for the estimation of  $\tau_{01}$  and  $\tau_{02}$ , respectively) derived from the equation proposed by Habibzadeh & Omid (2009) and valid for clear water conditions and large relative submergence ranges, including that tested in the present paper. Therefore,  $\beta$  values were computed using Eq. (2b). According to Hughes & Flack (1984), Ead &

Rajaratnam (2002) and Carollo et al. (2007),  $\beta$  is depending on the relative roughness.

The analysis of the experimental results shows that  $\beta$  values can be satisfactorily approximated by the following best-fit equation ( $R^2=0.8$ ):

$$\beta = -0.14 \left( 1 - e^{-\frac{2.38 d_{50}}{k}} \right) \quad (6)$$

where  $k$  is the critical depth and  $d_{50}$  is the mean diameter of the channel bed material. Note that for smooth bed  $\beta=0$ .

Combining Eq. (3), Eq. (5) and Eq. (6), the general expression of the sequent depth ratio can be obtained as:

$$Y = 0.5 \left( -1 + \sqrt{1 + 8 \left( 3.32^{1.52i} F_1 \right)^2 \left[ 1 + 0.14 \left( 1 - e^{-\frac{2.38 d_{50}}{k}} \right) \right]} \right) \quad (7)$$

and it is valid for both smooth and rough beds. Note that for  $i=0$  and  $d_{50}=0$  m (horizontal smooth bed), Eq. (7) coincides with Bélanger's equation. In addition, for  $d_{50}=0$  m and  $0.25 \leq i \leq 0$ , Eq. (7) coincides with the relationship proposed by Pagliara & Peruginelli (2000), thus it well predicts all the data for hydraulic jumps occurring on adverse-sloped smooth beds.

For rough bed conditions, Eq. (7) was validated using experimental data derived from the literature (for horizontal rough beds) and conducting selected experimental tests for  $i=-0.1$ . Thus, Eq. (7) is valid in the following ranges of parameters:  $-0.1 \leq i \leq 0$  and  $0 \leq d_{50}/k \leq 0.5$ . Finally, it can be noted that both the integrated shear stress and  $\beta$  increase with the relative roughness.

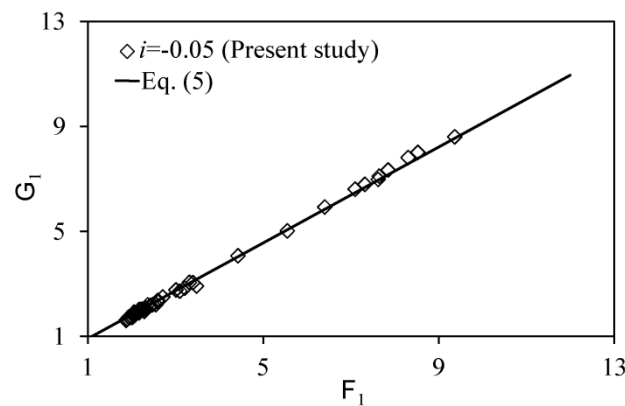


Figure 3  $G_1(F_1)$  for rough beds and  $i=-0.05$

## 4. Results

### 4.1. Sequent depth ratio

Experimental data were analysed and the proposed Eq. (7) was tested for different relative roughness and bed slope values. In addition, a comparison between smooth and rough configurations was conducted to highlight the effect of roughness on the main hydraulic jump characteristics. Experimental data were plotted along with Eq. (7) and they were grouped according to channel bed slope  $i$  and relative roughness  $d_{50}/k$ . Five relative roughness ranges were distinguished:  $0 < d_{50}/k < 0.1$ ,  $0.1 < d_{50}/k < 0.2$ ,  $0.2 < d_{50}/k < 0.3$ ,  $0.3 < d_{50}/k < 0.4$  and  $0.4 < d_{50}/k < 0.5$ . Note that for smooth bed  $d_{50}/k=0$ .

Present study data were compared with those derived from both Pagliara & Peruginelli (2000) (for the same channel slopes, i.e.,  $i=-0.05$  and  $-0.1$ ) and Pagliara et al. (2008) (for the same bed materials, relative roughness ranges and channel slope  $i=0$ ). In Eq. (7),  $d_{50}/k$  was assumed as the mean value of the considered range (e.g.,  $d_{50}/k=0.25$  for  $0.2 < d_{50}/k < 0.3$ ).

Figure 4a reports experimental data relative to both rough beds (with  $0 < d_{50}/k < 0.1$ ,  $i=0$  and  $i=-0.05$ ) and smooth adverse-sloped beds ( $i=-0.05$ ), along with the corresponding plots of Eq. (7). For the same approaching  $F_1$ , the sequent depth ratio  $Y$  decreases with relative roughness, confirming the findings of all previous cited studies. In addition, it can be noted that for both slope values, the corresponding plots of Eq. (7) for rough beds are very close to those for smooth beds. This is due to the fact that the mean relative roughness ( $d_{50}/k=0.05$ ) is close to 0, therefore the phenomenon is very similar to that occurring on smooth beds.

Furthermore,  $Y$  values are slightly over-estimated by Eq. (7) for high Froude numbers, as also observed by Harleman (1959) for smooth beds, and by Pagliara et al. (2008) and Carollo et al. (2007) for horizontal rough beds and small relative roughness (closest condition to that relative to smooth beds). This occurrence does not happen for higher relative roughness and for both horizontal and adverse-sloped beds. Figure 4b-c shows experimental data for  $0.2 < d_{50}/k < 0.3$  and  $0.4 < d_{50}/k < 0.5$ , and  $i=0$  and  $-0.05$ , along with the corresponding plots of Eq. (7).  $Y$  decreases with relative roughness, for both horizontal and adverse-sloped beds. In addition, for higher relative roughness, Eq. (7) well predicts data trend also for higher  $F_1$ .

Figure 4d shows the comparison of the experimental data for rough beds and  $i=-0.05$ , grouped for different relative roughness ranges, along with the respective plots of Eq. (7). Except for higher  $F_1$ ,  $Y$  decreases with relative roughness, with all other parameters being constant.

Selected experiments were also conducted to validate Eq. (7) for  $i=-0.1$  and rough beds. Figure 4e shows the comparison of data relative to experimental tests with smooth beds for  $i=-0.05$  and  $i=-0.1$  with those relative to rough bed for  $i=-0.1$ . Equation (7) satisfactorily

predicts all experimental data. In addition,  $0.1 < d_{50}/k < 0.2$  and  $i = -0.1$ , thus for  $d_{50}/k > 0.1$ , the peculiar trend of  $Y$  observed for higher  $F_1$  and for both smooth and low relative roughness beds (see Fig. 4a) is no more evident. Figure 4f shows the comparison between measured and calculated (with Eq. 7)  $Y$  values for rough beds and  $-0.1 \leq i \leq 0$ , including data derived from Pagliara et al. (2008). It can be easily noted that Eq. (7) furnishes a reasonably good estimation of the sequent depth ratios. Finally, the data derived from other authors' studies were taken into consideration to test the predictive capability of the proposed Eq. (7). The comparison between measured and calculated values of the variable  $Y$  is shown in Fig. 5a-b for both rough and smooth beds, respectively.

Figure 5a shows the comparison between measured  $Y$  values from Hughes & Flack (1984) and Carollo et al. (2007) for rough horizontal beds with the corresponding values computed using Eq. (7). Figure 5b shows the same for the data from Okada & Aki (1955), Hughes & Flack (1984), McCorquodale & Mohamed (1994), Pagliara & Peruginelli (2000) and Carollo et al. (2007) for smooth beds (horizontal and adverse-sloped). For rough beds Eq. (7) is slightly overestimating sequent depth ratios (mostly for higher  $F_1$  values). This can be due to the fact that experimental data derived by other authors were obtained without taking into consideration the air concentration. In other words, the systematic deviation between the data from previous studies and those predicted by Eq. (7) is due to the fact that air concentration increases with  $F_1$ , as also observed by Pagliara, Roshni, & Carnacina (2009). Nevertheless, considering the complexity of the phenomenon, the predictive performance of Eq. (7) appears reasonably accurate.

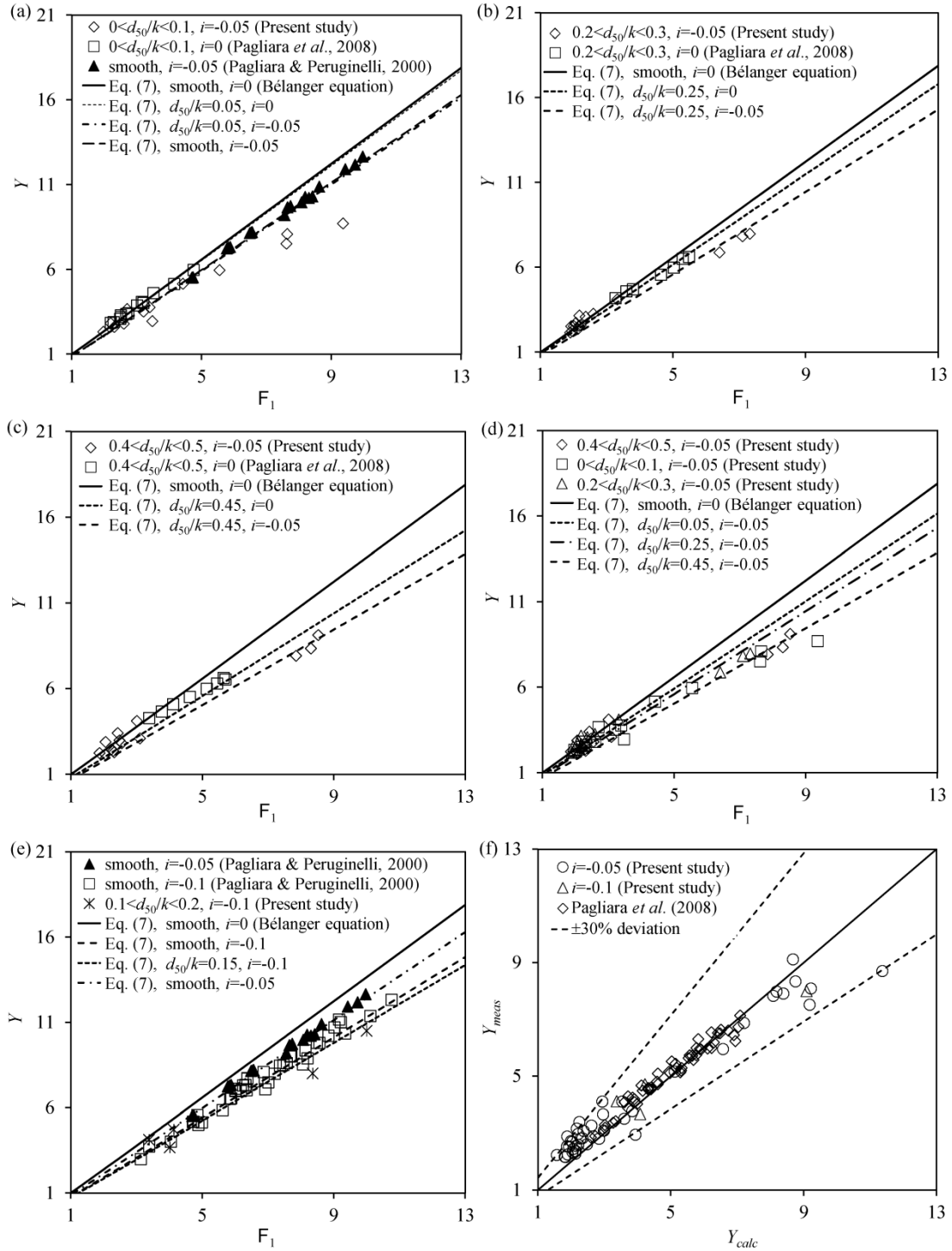


Figure 4 Experimental data and Eq. (7) for  $Y(F_1)$ : (a)  $-0.05 \leq i \leq 0$  and  $0 < d_{50}/k < 0.1$  including data for smooth adverse-sloped beds; (b)  $-0.05 \leq i \leq 0$  and  $0.2 < d_{50}/k < 0.3$ ; (c)  $-0.05 \leq i \leq 0$  and  $0.4 < d_{50}/k < 0.5$ ; (d)  $-0.05 \leq i \leq 0$  and  $0 < d_{50}/k < 0.5$ ; (e)  $-0.1 \leq i \leq -0.05$  and  $0.1 < d_{50}/k < 0.2$  including data for smooth beds; (f) comparison between measured and calculated (with Eq. 7) values of  $Y$  for rough beds and  $-0.1 \leq i \leq 0$

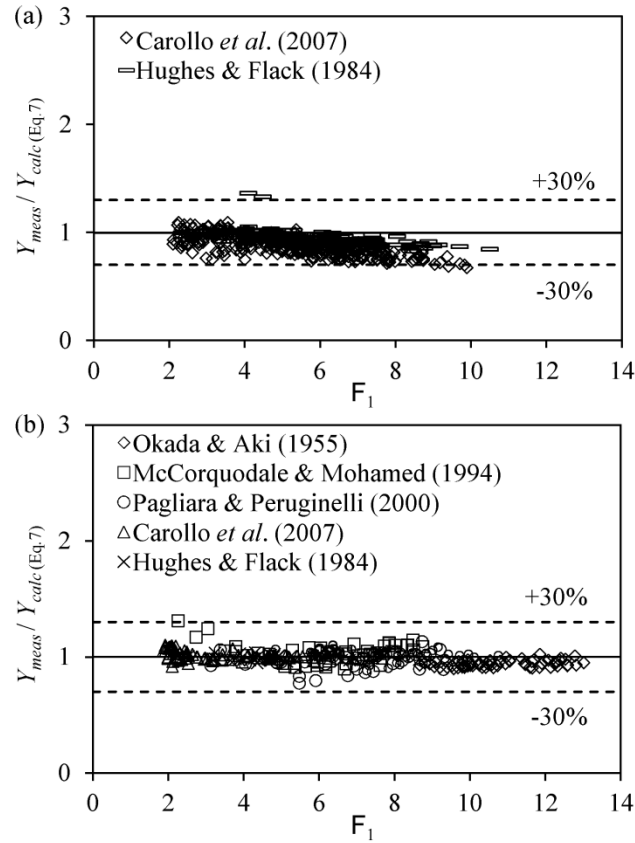


Figure 5 The ratio  $Y_{meas} / Y_{calc(Eq.7)}$  as a function of  $F_1$  for (a) rough beds and (b) smooth beds

#### 4.2. Roller length

Another important parameter is the roller length. In the case of adverse-sloped beds (both smooth and rough), the roller length is assumed to be the hydraulic jump length (McCorquodale & Mohamed, 1994; Okada & Aki, 1955; Pagliara & Peruginelli, 2000). According to Carollo et al. (2007) and Pagliara et al. (2008), the roller length  $L_r$  is depending on the relative roughness.

Carollo et al. (2007) proposed a relationship by which the non-dimensional roller length  $L_r/y_1$  can be satisfactorily estimated using Eq. (8), which was also validated using experimental data derived from other authors (Hughes & Flack, 1984; Hager, Bremen, & Kawagowshi, 1990):

$$\frac{L_r}{y_1} = 4.616 \left( \frac{y_2}{y_1} - 1 \right) \quad (8)$$

Equation (8) was also adopted in the present study and it was validated in the tested range of parameters. Note that both the roughness and bed slope are indirectly included in Eq. (8), as the sequent depth ratio was estimated by using Eq. (7). In addition, data derived from other

studies (including smooth adverse-sloped bed) were also taken into consideration, as shown in Fig. 6.

Considering the complexity of the phenomenon, Eq. (8) furnishes a good estimation of the non-dimensional roller length. Therefore, its validity can be extended to the following ranges of parameters:  $-0.2 \leq i \leq 0$ ,  $0 \leq d_{50}/k < 0.5$ .

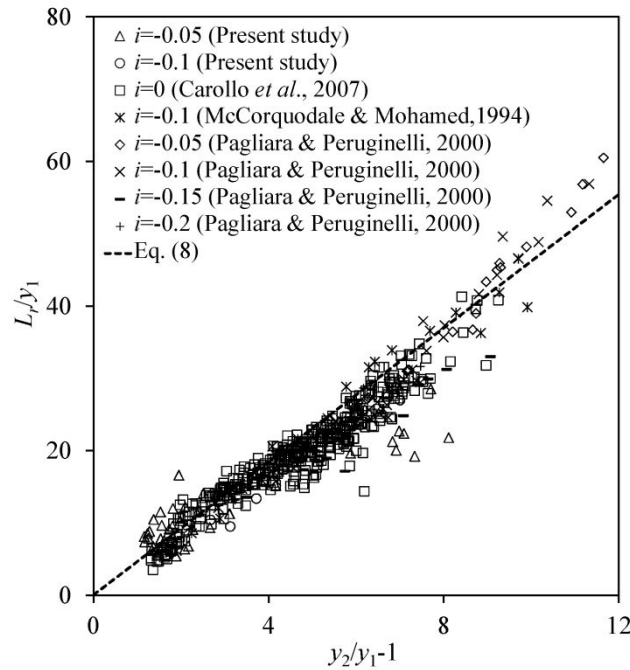


Figure 6 The ratio  $L_r/y_1$  as a function of  $(y_2/y_1 - 1)$  for smooth and rough beds for  $-0.2 \leq i \leq 0$

#### 4.3. Observations on air concentration profiles

In this study, air concentration profiles were measured both in section 1 (upstream) and section 2 (downstream) of the hydraulic jump. Air concentration measurements were used to estimate the effective (equivalent) water depths. In the following, a qualitative analysis of the air concentration profiles is proposed for all of the tested materials and for bed slope  $i = -0.05$ .

A similar analysis was also conducted by Pagliara et al. (2009) in the case of a block ramp, whose slope was  $i = 0.275$  (positive). The authors observed that the air concentration profiles are significantly influenced by the relative equivalent depth  $d_e/d_{84}$  (the ratio between effective depth and a characteristic diameter of base material). They showed that air concentration increases when  $d_e/d_{84}$  decreases. This is mainly due to both the presence of drag and shear vortices between the stones and an increasing interaction between the free surface and the stones. Furthermore, streamwise oriented vortexes were also visible and were more stable for low relative flow depth. This effect was also observed in the case of adverse-sloped

beds, in particular close to section 1, where macro-roughness flow conditions take place. The described behaviour is also highlighted in Fig. 7a, in which air concentration profiles, relative to sections 1 and 2 and base material *E2*, are shown. In addition, the effect of the base material on air concentration profiles at section 2 is shown in Fig. 7b where the comparison between profiles for *E2*, *E3* and *E4* is reported. Even if a certain increasing trend in air concentration is visible due to the material size variation, the difference between the average non-dimensional profiles is slight.

Based on these observations, it can be concluded that the material size affects the estimation of flow depths mainly in macro-roughness conditions. In other words, water depths at section 1 are more influenced by air entrainment than the corresponding depths at section 2.

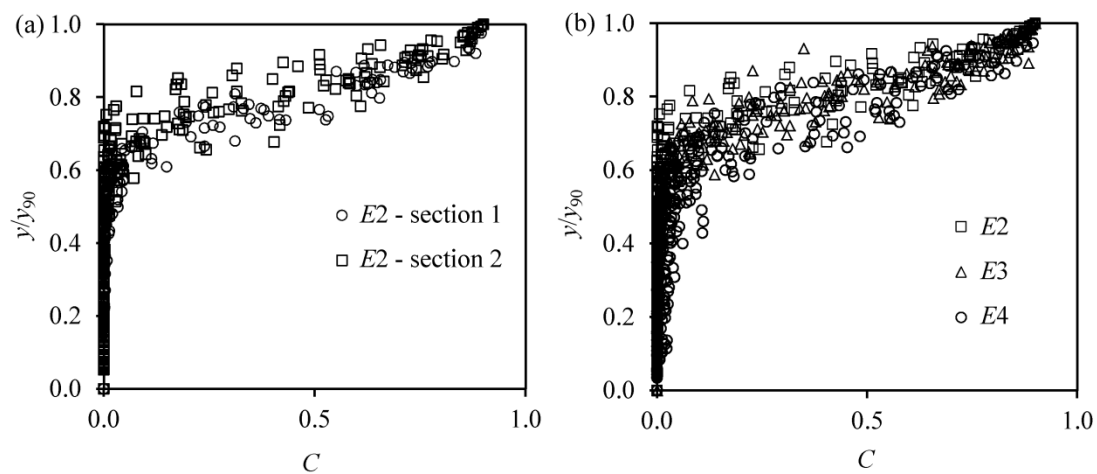


Figure 7 Air concentration profiles for (a) sections 1 and 2 and material *E2* and (b) section 2 and materials *E2*, *E3*, *E4*

## 5. Discussion

The present study confirmed that the hydraulic jump sequent depth decreases with increasing boundary roughness. It is worth noting that the methodology proposed by Hughes & Flack (1984) to locate the effective top does not affect the results. In fact, Hughes & Flack (1984) analyzed the potential error introduced in the results due to the estimation of the *ET* and concluded that “the error is not as large as might be expected because of the manner in which it affects  $y_2/y_1$  versus  $F_1$  diagram”. For example, they proved that a change in the virtual bottom level of  $\pm 20\%$  results in a  $\pm 5\%$  change in the relationship  $y_2/y_1(F_1)$ .

A clear explanation of the hydraulic jump sequent depth reduction was furnished by Ead & Rajaratnam (2002). The authors analyzed the velocity field in correspondence with hydraulic jumps showing that the intense mixing induced by the bed roughness results in significant Reynolds shear stresses and in prominent reduction of the velocity field above the

rough bed. In other words, the reduction of the sequent depth on rough bed is essentially due to the increase of bed shear stresses.

Air entrainment is a delicate topic in physical scale model testing due to scale effects and it requires a more detailed discussion. In the studies of hydraulic jumps, generally, the Froude similitude is adopted, resulting in smaller model Reynolds numbers than in prototypes. Therefore, scale effects may affect the two-phase flow properties. In particular, the scale effects on the air entrainment process in hydraulic jumps remains poorly understood (Chanson, 2008; Chanson, 2009). Chanson (2009) conducted a detailed experimental investigation on the topic analyzing both the dynamic similarities and scale effects for turbulent air-water flows in hydraulic structures. His analysis mainly focused on hydraulic jumps occurring in horizontal smooth channels, therefore the model configuration was quite different from that tested in the present study. Nevertheless, some significant insights can be found both in Chanson (2009) and Heller (2011) that may be beneficial in understanding how scale effects may affect the proposed results. Namely, both Chanson (2009) and Heller (2011) showed that the relative channel width has no significant effect on air-water flow properties for  $B/y_1 > 10$ , where  $B$  is the channel width. For the present study, this limitation is valid for most of the experimental tests. In fact, just a few tests are characterized by  $8 < B/y_1 < 10$ , whereas most of the experiments were conducted for  $B/y_1 > 10$ . In addition, Chanson & Murzyn (2008) showed that Reynolds number effects on the two-phase flow properties are more prominent in the developed shear layer (especially in terms of bubble count rate distribution). They noted a more rapid de-aeration of the jump roller with decreasing Reynolds number and an absence of self-similarity of the void fraction profiles in the developing shear layer for  $Re < 40000$ . In the present study, Reynolds numbers were much larger than 40000 and it was experimentally observed that the differences between the non-dimensional air concentration profiles were relatively slight for all of the tested hydraulic conditions and channel bed configurations. Therefore, although the model configurations tested are different from those analyzed by Chanson & Murzyn (2008) and Chanson (2009), based on the previous observations it can be concluded that for the present study scale effects are not significantly affecting the characteristic lengths of the hydraulic jumps (sequent depth ratios and roller length).

## 6. Conclusions

A new approach was developed to analyse the main features of a hydraulic jump under both rough and negative bottom slope conditions including the effect of air concentration. A semi-theoretical model was proposed to estimate both the sequent depth and the roller length in a wide range of geometric and boundary configurations. The increase of Reynolds shear

stresses induced by the bed roughness causes a reduction of the sequent depth ratio. The reduction is more prominent when increasing relative roughness and bed slope. The predicting capability of the proposed relationships was validated by conducting ad hoc experimental tests and by testing them with data obtained in the previous studies. The obtained results may be valuable for future theoretical work and practical applications as they relate to the hydraulic jump features under a wide range of hydraulic and boundary conditions.

### Notation

$B$  = channel width (m)

$C$  = air concentration (-)

$C_m$  = depth-average void fraction (-)

$d_e$  = equivalent/effective flow depth (m)

$d_{xx}$  = size of the base material for which xx% is finer (m)

$f_1$  = friction factor (section 1) (-)

$f_2$  = friction factor (section 2) (-)

$F_1 = U_1/(gy_1)^{0.5}$  approach Froude number (-)

$F_\tau$  = integrated shear stress per unit width ( $\text{N m}^{-1}$ )

$g$  = gravity acceleration ( $\text{m s}^{-2}$ )

$G_1$  = adverse jump parameter (-)

$i$  = channel bed slope (-)

$k$  = critical depth (m)

$k_s = d_{65}$  grain roughness height (m)

$K$  = coefficient for the determination of the weight (-)

$L$  = hydraulic jump length (m)

$L_r$  = length of roller (m)

$M_1 = \rho y_1 U_1^2$  momentum flux per unit width at section 1 ( $\text{N m}^{-1}$ )

$M_2 = \rho y_2 U_2^2$  momentum flux per unit width at section 2 ( $\text{N m}^{-1}$ )

$P_1 = 0.5\gamma_1^2 \cos\alpha$  hydrostatic force per unit width at section 1 ( $\text{N m}^{-1}$ )

$P_2 = 0.5\gamma_2^2 \cos\alpha$  hydrostatic force per unit width at section 2 ( $\text{N m}^{-1}$ )

$U_1$  = average velocity at section 1 ( $\text{m s}^{-1}$ )

$U_2$  = average velocity at section 2 ( $\text{m s}^{-1}$ )

$x$  = longitudinal coordinate (m)

$y$  = vertical coordinate (m)

$Y = y_2/y_1$  sequent depth ratio (-)

$y_1$  = effective upstream depth of the hydraulic jump (m)

$y_2$  = effective downstream depth of the hydraulic jump (m)

$y_{90}$  = distance normal to the bed where the air concentration  $C=90\%$  (m)

$W = 0.5\gamma LK(y_1+y_2)$  weight of the water in the control volume per unit width ( $\text{N m}^{-1}$ )

$\alpha$  = angle of the bed slope respect to horizontal (rad)

$\beta$  = parameter related to momentum deficit (-)

$\gamma$  = specific weight ( $\text{N m}^{-3}$ )

$\rho$  = water density ( $\text{kg m}^{-3}$ )

$\lambda = L_r/y_1$  non-dimensional length of roller (-)

$\sigma = (d_{84}/d_{16})^{0.5}$  material non-uniformity coefficient (-)

$\tau_{01}$  = shear stress at the upstream section of the hydraulic jump ( $\text{N m}^{-2}$ )

$\tau_{02}$  = shear stress at the downstream section of the hydraulic jump ( $\text{N m}^{-2}$ )

$\tau_{0\text{mean}}$  = mean value of the boundary shear stress ( $\text{N m}^{-2}$ )

## References

- Afzal, N., Bushra, A., & Seena, A. (2011). Analysis of turbulent hydraulic jump over transitional rough bed of a rectangular channel: universal relations. *Journal of Hydraulic Engineering*, 137(12), 835-845.
- Bakhmeteff, B. A. (1932). *Hydraulics of Open Channels*. New York: McGraw-Hill.
- Bhuiyan, F., Habibzadeh, N., Rajaratnam, N., & Zhu, D. Z. (2011). Reattached turbulent submerged offset jets on rough beds with shallow tailwater. *Journal of Hydraulic Engineering*, 137(12), 1636-1648.
- Carollo, F. G., Ferro, V., & Pampalone, V. (2007). Hydraulic jump on rough beds. *Journal of Hydraulic Engineering*, 133(9), 989-999.
- Carollo, F. G., Ferro, V., & Pampalone, V. (2009). New solution of classical hydraulic jump. *Journal of Hydraulic Engineering*, 135(6), 527-531.
- Chanson, H., & Murzyn, F. (2008). Froude similitude and scale effects affecting air entrainment in hydraulic jumps. *Proceedings of the World Environmental and Water Resources Congress 2008*, 1-10.
- Chanson, H. (2009). Turbulent air-water flows in hydraulic structures: dynamic similarity and scale effects. *Environmental Fluid Mechanics*, 9(2), 125-142.

- Ead, S. A., & Rajaratnam, N. (2002). Hydraulic jumps on corrugated beds. *Journal of Hydraulic Engineering*, 128(7), 656-663.
- Gill, M. A. (1980). Effect of boundary roughness on hydraulic jump. *International Water Power & Dam Construction*, 32(1), 22-24.
- Jan, C. D., & Chang, C. J. (2009). Hydraulic jumps in an inclined rectangular chute contraction. *Journal of Hydraulic Engineering*, 135(11), 949-958.
- Habibzadeh, A., & Omid, M. H. (2009). Bedload resistance in supercritical flow. *International Journal of Sediment Research*, 24(4), 400-409.
- Hager, W. H., & Bretz, N. V. (1988). Sill controlled stilling basin. Proceedings of the *International Symposium on Hydraulics for High Dams*, 273-280.
- Hager, W. H., Bremen, R., & Kawagowshi, N. (1990). Classical hydraulic jump: Length of roller. *Journal of Hydraulic Research*, 28(5), 591-608.
- Harleman, D. R. F. (1959). Discussion of "Turbulence characteristics of the hydraulic jump" by Rouse, H., Siao, T. T., & Nagaratnam, S., *Transactions ASCE*, 124, 959-962.
- Heller, V. (2011). Scale effects in physical hydraulic engineering models. *Journal of Hydraulic Research*, 49(3), 293-306.
- Hughes, W. C., & Flack, J. E. (1984). Hydraulic jump properties over a rough bed. *Journal of Hydraulic Engineering*, 110(12), 1755-1771.
- Leutheusser, H. J., & Kartha, V. C. (1972). Effects of inflow condition on hydraulic jump. *Journal of Hydraulic Division*, 98(8), 1367-1383.
- Leutheusser, H. J., & Schiller, E. J. (1975). Hydraulic jump in a rough channel. *International Water Power & Dam Construction*, 27(5), 186-191.
- McCorquodale, J. A., & Khalifa, A. (1983). Internal flow in hydraulic jumps. *Journal of Hydraulic Engineering*, 109(5), 684-701.
- McCorquodale, J. A., & Mohamed, M. S. (1994). Hydraulic jumps on adverse slopes. *Journal of Hydraulic Research*, 32(1), 119-130.
- Okada, A., & Aki, S. (1955). Experimental study of hydraulic jump on reversed slope apron. *Journal of Central Research Institute of Electric Power Industry Technical Lab*, 5(6).
- Ohtsu, I. (1981). Forced hydraulic jump by a vertical sill. *Transactions of the Japan Society of Civil Engineers*, 13, 165-168.
- Ohtsu, I., Yasuda, Y., & Yamanaka, Y. (1991). Drag on vertical sill of forced jump. *Journal of Hydraulic Research*, 29(1), 29-47.
- Pagliara, S., & Peruginelli, A. (2000). Limiting and sill-controlled adverse-slope hydraulic jump. *Journal of Hydraulic Engineering*, 126(11), 847-851.
- Pagliara, S., Lotti, I., & Palermo, M. (2008). Hydraulic jumps on rough bed of stream rehabilitation structures. *Journal of Hydro-Environment Research*, 2(1), 29-38.

- Pagliara, S., Roshni, T., & Carnacina, I. (2009). Aeration and velocity profile over block ramp elements. *Proceedings of the 33<sup>rd</sup> IAHR Congress*, 4925-4932.
- Pagliara, S., Carnacina, I., & Roshni, T. (2010). Air-water flows in the presence of staggered and row boulders under macroroughness conditions. *Water Resources Research*, 46, 1-11.
- Paterka, A. J. (1983). *Hydraulic Design of Stilling Basins and Energy Dissipators* (Report No. 25). Denver: US Dept. of the Interior, Bureau of Reclamation, Engineering Monograph.
- Rajaratnam, N. (1965). The hydraulic jump as a wall jet. *Journal of Hydraulic Division*, 91(5), 107-132.
- Rajaratnam, N. (1966). The hydraulic jump in sloping channels. *Irrigation and Power*, 32(2), 137-149.
- Rajaratnam, N. (1967). Hydraulic jumps. *Advances in hydroscience* (pp. 197-280), San Diego: Academic.
- Stevens, C. J. (1942). Discussion of "The hydraulic jumps in sloping channels". *Transactions ASCE*, 2228, 1125-1135.
- Wu, S., & Rajaratnam, N. (1995). Free jumps, submerged jumps and wall jets. *Journal of Hydraulic Research*, 33(2), 177-212.